## ORIGINAL RESEARCH



# The influence of pre-fibrillation via planetary ball milling on the extraction and properties of chitin nanofibers

Tuhua Zhong · Michael P. Wolcott · Hang Liu · Nathan Glandon · Jinwu Wang ©

Received: 23 December 2019/Accepted: 23 April 2020

© This is a U.S. Government work and not under copyright protection in the US; foreign copyright protection may apply 2020

**Abstract** A planetary ball milling was applied as a pretreatment of chitin powder to prepare precursors for chitin nanofiber (ChNF) production. The study aims to examine the effects of ball milling conditions (dry milling, and wet milling in neutral and acidic aqueous medium) on the degree of pre-fibrillation of the ChNF precursors and the characteristics of the resulting nanofibers. The results showed that no fibrous-morphology ChNFs were obtained using dry ball milling followed by high-pressure

**Electronic supplementary material** The online version of this article (https://doi.org/10.1007/s10570-020-03186-7) contains supplementary material, which is available to authorized users.

T. Zhong · M. P. Wolcott (⊠) · H. Liu Composite Materials and Engineering Center, Washington State University, Pullman, WA 99164, USA e-mail: wolcott@wsu.edu

H. Liu Apparel, Merchandising, Design and Textiles, Washington State University, Pullman, WA 99164, USA

Published online: 14 May 2020

Department of Chemical Engineering, Artie McFerrin, Texas A&M University, College Station, TX 77843, USA

J. Wang (⊠)
Forest Products Laboratory, U.S. Forest Service, Madison, WI 53726, USA
e-mail: jinwu.wang@usda.gov

homogenization (HPH), but fibrous-morphology ChNFs were successfully prepared using wet ball milling as a pretreatment. Ball milling in a mildly acidic aqueous medium was found to most effectively pre-fibrillate chitin, thus facilitating fibrillation in the subsequent HPH treatment to generate the finest ChNFs with an average diameter of around 12 nm and the narrowest size distribution. The resultant chitin products from wet milling pretreatment exhibited much higher crystallinity and thermal stability than those from dry milling. The results suggest that pre-fibrillation of chitin via ball milling in this study plays a crucial role in the successful procuration of the ChNFs in a subsequent mechanical disintegration process, while wet ball milling, especially under mildly acidic conditions, is a promising green approach to produce efficient precursors for ChNF production.

 $\begin{tabular}{ll} \textbf{Keywords} & Ball milling \cdot Pre-fibrillation \cdot \\ Crystallinity \cdot Chitin nanofibers \cdot Particle size \cdot \\ Thermal property \end{tabular}$ 

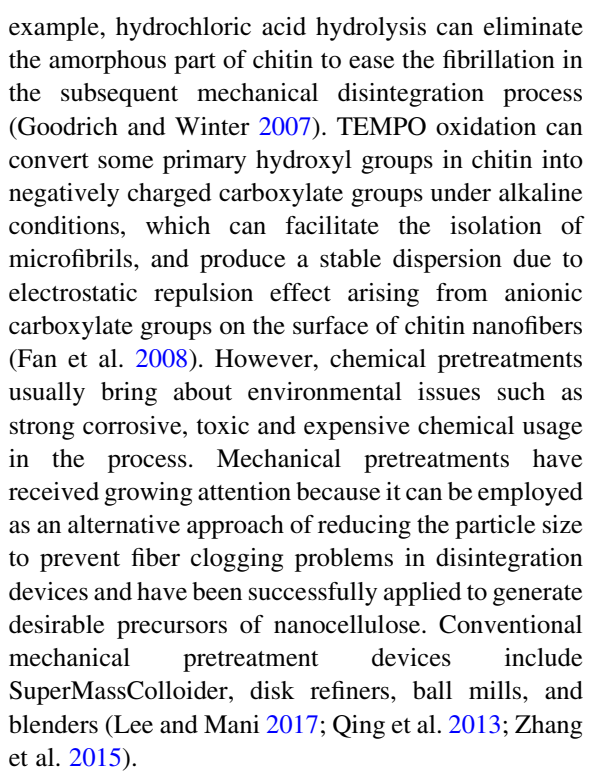
#### Introduction

Chitin is an abundant but still underutilized polysaccharide that exists in crustaceans, fungi, and insects. It is biosynthesized every year at a rate of  $10^{10}$  to  $10^{11}$ 



tons (Kumar 2000; Nair and Dufresne 2003). Chitin can be categorized into  $\alpha$ -,  $\beta$ - and  $\gamma$ -chitin on the basis of the arrangement of chitin molecule chains (Rinaudo 2006). α-Chitin is the most ubiquitous and can be extracted from crab, shrimp, and lobster shells. Around 6 to 8 million tonnes are projected to be generated globally every year and most of them have been largely regarded as food waste from the canning industry (Rinaudo 2006; Yan and Chen 2015). Chitin occurs in the form of microfibrils of long-chains of the N-acetylglucosamine polymer on the nanoscale that are fundamental supporting units within the structure in the crustaceans, fungi, and yeast (Pillai et al. 2009; Rinaudo 2006; Salaberria et al. 2015). The extraction of these microfibrils as chitin nanofibers (ChNFs) has been extensively studied because of their advanced properties. Namely, ChNFs possess a high specific area, high strength and stiffness, but low density. advantages Additional include renewability, biodegradability, and biocompatibility, which allow for their use as sustainable functional fillers such as reinforcements and antimicrobial agents for biopolymers or synthetic polymers (Butchosa et al. 2013; Ifuku et al. 2011; Li et al. 2015; Salaberria et al. 2015; Shams et al. 2011; Zhong et al. 2019).

The ChNF extraction usually demands intensive mechanical disintegration using conventional disintegration devices such as intense ultrasonication, highpressure homogenization, microfluidization, and ultrafine grinding (Qing et al. 2013). In particular, highpressure homogenization is regarded as one of the most effective ways because it can generate strong mechanical shearing forces acting on fibers entrained inflows with high velocity under high pressure in a microchannel to initiate the fibrillation of the fibers (Missoum et al. 2013). However, chitin is aggregates of microfibrils formed by intermolecular hydrogen bonding, which makes it challenging in disintegrating chitin fibers into nanofibrils. Moreover, bulk particle size and fiber agglomeration often result in clogging in the microchannel in disintegration devices, leading to the premature termination of the production process (Zhang et al. 2015). Because of these issues, pretreatments are often applied prior to the mechanical disintegration process. Chemical pretreatments are effective approaches due to their low energy consumption, including strong acid hydrolysis (Goodrich and Winter 2007) and (2,2,6,6-Tetramethylpiperidin-1-yl)oxyl (TEMPO) oxidation (Fan et al. 2008). For



Different mechanical pretreatments have also been attempted to pretreat chitin for ChNF production, including the use of an Ultra-Turrax homogenizer (Salaberria et al. 2015) and domestic blender followed by ultrafine grinding in a SuperMassColloider (Ifuku et al. 2010). One unexplored method among mechanical pretreatments of chitin for ChNF production is ball milling. Ball milling has been accepted as a routine pretreatment process for various materials for particle size reduction due to its simplicity, use of relatively inexpensive equipment, and versatility (Nemoto et al. 2017; Zhang et al. 2015). Ball milling has also been used as a powerful tool to alter the crystal structure and crystallinity for different materials such as inorganic materials (Chauruka et al. 2015; Venkataraman and Narayanan, 1998), biopolymers (Lu et al. 2015), and organic substances (Willart and Descamps 2008). De-crystallization of cellulosic or chitin materials may be beneficial for downstream biorefinery processes, i.e., subsequent enzymatic degradation for low molecular organic materials production. Conversely, the deconstruction of crystal structure and the reduced crystallinity may be unwanted in ChNF production because de-crystallization can adversely affect the mechanical and thermal properties of final products (Nakagawa et al. 2011;



Pedersoli Júnior 2000; Zhang et al. 2015). To date, little attention has been paid to the selection of a planetary ball milling to pretreat chitin for ChNF production, the effect of planetary ball milling on the properties of ChNF precursors and resultant products remain unstudied.

In this study, the objective was to investigate the effects of various ball milling conditions (dry milling, and wet milling in neutral or mildly acidic conditions) on the degree of pre-fibrillation and the properties of ChNF precursors. The particle size, size distribution, microstructure, and crystallinity after ball milling were investigated. Our study also explored ChNF preparation through mechanical disintegration of ball milling-pretreated chitin particles in a high-pressure homogenizer and then characterized the resultant ChNFs including morphology, size, and thermal stability.

# **Experimental**

## Materials

Chitin from shrimp shells (powder, practical grade) was purchased from Sigma-Aldrich. Acetic acid (glacial, ACS grade) was purchased from EMD Millipore Corporation. Potassium bromide (KBr) was purchased from Sigma-Aldrich.

# Methods

Mechanical pretreatment of chitin using dry ball milling (DBM)

The chitin was milled in two stainless steel jars at a rotation speed of 645 RPM for 120 min using a 4-Station Planetary Ball Mill (PQ-N04, Across International, USA). Each jar (100 cm<sup>3</sup>) contained chitin powder (3 g, 4% moisture content) and stainless grinding balls (90 g total weight: 14 large balls of 10 mm in diameter and 38 small balls of 6.25 mm in diameter) The dry ball milled chitin was labeled as the DBM sample.

Mechanical pretreatment of chitin using wet ball milling (WBM)

Neutral wet ball milling of chitin was conducted in two jars in a similar manner to the dry milling. Each jar contained a "paste-like" mixture of chitin powder (3 g), distilled water (15 g), and grinding balls (90 g). The milled chitin sample was coded as pH7/WBM. Chitin was also milled in a mildly acidic aqueous medium using a slightly modified procedure from the neutral wet milling. Chitin particle suspension was first created by mixing chitin powder (3 g) with water (100 g). Glacial acetic acid was then added dropwise until the pH reached 3. The suspension was vacuum filtrated to remove excess water until the weight of the "paste-like" chitin was 18 g was obtained, i.e. the chitin to water weight ratio was maintained to be the same as that for the neutral wet milling as 3 g/15 g. The acidified chitin was ball-milled in the same way as used for milling the pH7/WBM. The sample was coded as pH3/WBM.

Mechanical disintegration using high-pressure homogenization (HPH)

The dry- and wet ball milled chitin particles were redispersed in water to adjust chitin concentration to be 0.5 wt%. One portion of the chitin particle suspensions was adjusted to pH = 3 by adding acetic acid. The ball milling-pretreated chitin particle suspensions ( $\sim 0.5$  wt%, pH = 3 or pH = 7) passed through a high-pressure homogenizer equipped with an 87- $\mu$ m diamond interaction chamber (LM20, Microfluidics, USA) 10 times under a pressure of 30,000 psi. Based on the various conditions (DBM, WBM, HPH, and pH = 3 or pH = 7) of milling pretreatment and mechanical disintegration treatment, five different samples were coded as DBM-pH7/HPH; DBM-pH3/HPH, and pH3/WBM-pH7/HPH; pH7/WBM-pH3/HPH, and pH3/WBM-pH3/HPH.

#### Particle size distribution measurement

The volume-based particle size and size distribution of chitin particles were measured with a laser scattering particle size analyzer (Mastersizer 3000, Malvern, UK) in duplicate. The average median particle size was used to represent the particle size for analysis.



Scanning electron microscopy (SEM)

The surface morphology of chitin particles was observed with an SEM (Quanta 200F, FEI, USA) at 20 kV. Dry chitin particles were scattered directly onto the carbon tape mounted to a metal stub. For chitin particles in water, the diluted suspensions were dropped to an aluminum film and dried overnight. All the samples were coated with platinum using a sputter prior to the SEM observation.

Transmission electron microscopy (TEM)

The morphology of the ChNFs was observed with a TEM (Tecnai G2 20 Twin, FEI, USA) operating at 200 kV. A 10-μL aliquot of the diluted dispersion was dropped onto a Formvar/ nickel grid, and then a drop of 2% uranyl acetate negative stain was added. The sample on the grid was dried overnight prior to the TEM observation.

X-ray diffraction (XRD) characterization

The diffractograms of ball-milled chitin particles were recorded using a Miniflex 600X-ray powder diffractometer (Rigaku, Japan) with a Cu K $\alpha$  X-ray source ( $\lambda = 0.1548$  nm) at 40 kV and 15 mA. Wet ball-milled chitin particles were freeze-dried before XRD characterization. The crystallinity index (CrI) was estimated using an empirical equation as described by Fan et al. (2008).

$$CrI = \frac{I_{110} - I_{amorphous}}{I_{110}} \times 100\%$$

where  $I_{II0}$  is the intensity of the main peak (110) and  $I_{amorphous}$  is the intensity of the amorphous portion at  $2\theta = 16.0^{\circ}$ .

Fourier-transformed infrared (FTIR) analysis

FTIR spectra of the resulting chitin products were recorded using an FTIR spectrometer (Nicolet iS-50, Thermo Fisher Scientific, USA) under transmission mode from 4000 cm<sup>-1</sup> to 400 cm<sup>-1</sup> with a 4 cm<sup>-1</sup> resolution and 64 scans. The pellets made of potassium bromide (KBr) and chitin samples at a weight ratio of 50:1 were prepared before the FTIR analysis.



The thermal stability of the resulting chitin products was assessed by a thermogravimetric analyzer (SDT Q600, TA, USA), with a temperature ramp-up rate of 10 °C/min and a nitrogen purging flow rate of 100 mL/min.

Zeta potential measurement

The zeta potential of the resulting chitin nanofibers in water (concentration: 0.1 wt%, pH = 3) was measured at room temperature using a Zetasizer Nano (Malvern, UK). The measurements were performed six times.

#### Results and discussion

Effects of ball milling conditions on particle size and size distribution of milled chitin

Milling conditions greatly influenced the particle size and size distribution of the resulting chitin particles. The dry milling dramatically reduced the size of the chitin particles from a median particle size of 142.8 μm to a median particle size of 13.8 μm, a roughly tenfold size reduction after the milling (Fig. 1a). The wet ball milling reduced the size of the chitin particles to a median size of 45.5 µm under the neutral condition (pH7/WBM) and 62.0 μm under the acidic condition (pH3/WBM), less pronounced than that under the dry milling. Generally, dry ball milling enables more direct contact between grinding media and raw materials than does wet ball milling. This led to the more frequent transfer of imposed stresses generated by mechanical milling to the materials, resulting in the cleavage of materials and ultimately particle size reduction. By contrast, lower impact and shear forces were expected in wet ball milling since the water medium likely acted as a buffer between the materials and grinding media. This can explain why the sizes of the particles from the wet ball milling were larger than that from the dry ball milling. It has been reported that chitin usually contains about 5–15% amino groups because partial deacetylation often occurs during the extraction from shells (Cárdenas et al. 2004; Pillai et al. 2009). Once these existing amino groups are cationized with the addition of an acid (Ifuku et al. 2010; Suenaga et al. 2017), interfibrillar electrostatic



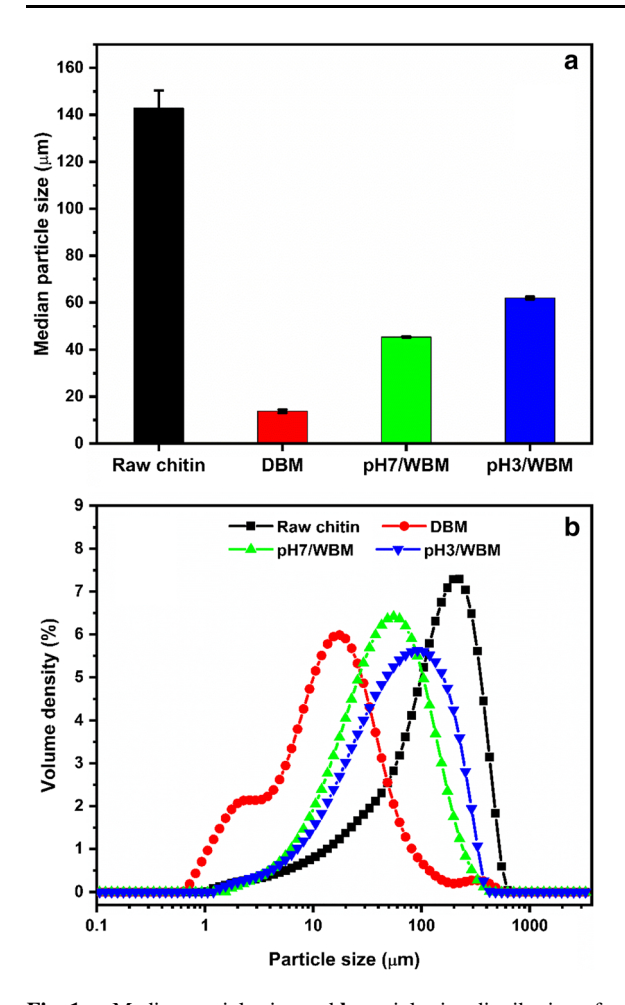


**Fig. 1** a Median particle size and **b** particle size distribution of raw chitin and the milled chitin particles

repulsion is generated, which would aid mechanical milling to effectively fibrillate packed microfibrils. These explain that the particles obtained by the wet milling in mildly acidic aqueous medium exhibited a slightly larger size than that from the neutral wet milling. As can be seen from Fig. 1b, the DBM sample had a trimodal distribution curve with two very small peaks located at around 300  $\mu$ m and 3  $\mu$ m, respectively. The wet ball milling produced relatively narrower unimodal distributions than did the dry ball milling.

Effect of ball milling conditions on crystal structure and crystallinity of milled chitin

Dry ball milling significantly altered the crystalline structure and crystallinity of chitin whereas wet ball milling had little effect on the crystal structure and crystallinity. As shown in Fig. 2, the raw chitin had six characteristic peaks in the XRD pattern at  $2\theta = 9.5^{\circ}$ , 12.8°, 19.3°, 20.9°, 23.4°, and 26.5°, which corresponded to the crystalline planes of (020), (021), (110), (120), (130), and (013), respectively, suggesting a typical crystalline structure of  $\alpha$ -chitin (Fan et al. 2008; Minke and Blackwell 1978). The values of the characteristic peak positions for all the milled chitin particles are presented in Table 1S. The average CrI of the raw chitin was approximate 90%. The DBM sample after the dry milling presents a broad reflection without the characteristic peaks, indicating the amorphization of the chitin by the dry milling. However, both pH7/WBM and pH3/WBM samples from the wet ball milling retained the characteristic peaks with an average CrI of around 87%, indicating that the wet milling did not alter the crystalline structure. As discussed previously, dry milling can impose many high stresses on chitin, thereby disrupting crystalline domains of chitin and decreasing the crystallinity. By contrast, wet milling had water to act as a good cushion between chitin domains to prevent the collapse of the crystal structure. These assumptions can explain why the wet milling preserved most of the crystallinity whereas the dry milling drastically reduced it.

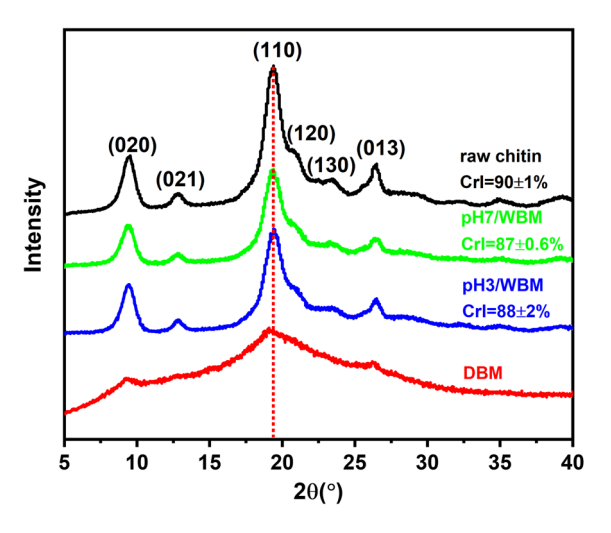


**Fig. 2** XRD patterns of raw chitin and the milled chitin particles and the corresponding crystallinity index (CrI)



Effect of ball milling conditions on particle morphology and microstructure of milled chitin

Raw chitin particles exhibited a flake-like shape (Fig. 3a) and were reduced to mostly smaller particles in a quasi-circular shape after the dry ball milling (Fig. 3c), but a small number of large chitin particles were also present. The SEM observation was consistent with the particle size analysis of the DBM sample as shown in Fig. 1b. Although the dry ball milling dramatically reduced particle sizes (Fig. 3c-d), it did not fibrillate the chitin at all. The DBM sample still exhibited a close-packed texture that was similar to that of the raw chitin (Fig. 3b). The particles produced by the wet ball milling under either the neutral or acidic conditions were in a flake-like shape (Fig. 3e and Fig. 3g), partially sheared apart into microfibril bundles, and somewhat loose and open (Fig. 3f and h). This might be attributed to the effect of the water that penetrated into the chitin particles, weakened hydrogen bonding between microfibrils, and swollen the chitin (Zhang et al. 2015). It assumed that the impact and shearing forces generated from the wet ball milling more easily acted on the water-swollen and softened chitin particles and separated them into microfibril bundles. In addition, the wet ball milling under the acidic condition produced particles with a higher degree of fibrillation than under the neutral condition. This more effective fibrillation could be ascribed to the electrostatic repulsion force among the cationized chitin fibers under the mildly acidic condition (Ifuku et al. 2010), which would weaken intermolecular forces and ease the liberation of microfibrils from their bundles as nanofibrils.

Effect of ball milling and mechanical disintegration conditions on morphology and size of chitin nanofibers

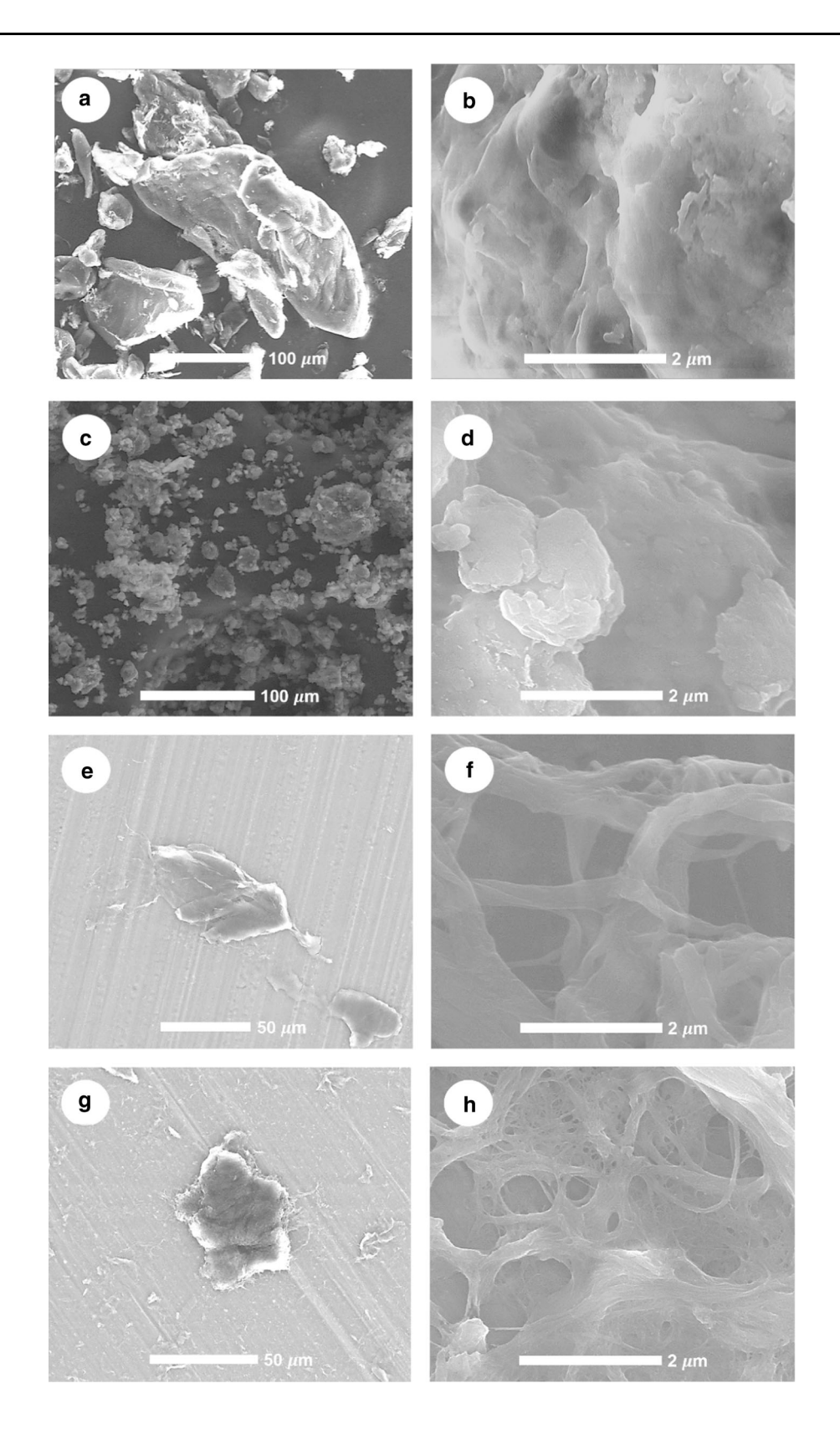
The high-pressure homogenization treatment reduced the particle sizes of the milled chitin particles further to a degree depending on both milling and homogenization conditions. The DBM-pH7/HPH and DBM-pH3/HPH samples obtained through the dry milling followed by the high-pressure homogenization retained their flake-like appearance (Fig. 4a, b). Their stable suspensions could not sustain over one month and the chitin particles gradually settled on the bottom (Fig. 4a, b insets). In addition, the acid condition

**Fig. 3** SEM images of raw chitin and the milled chitin particles. ► (**a**-**b** raw chitin; **c**-**d** DBM; **e**-**f** pH7/WBM; and **g**-**h** pH3/WBM)

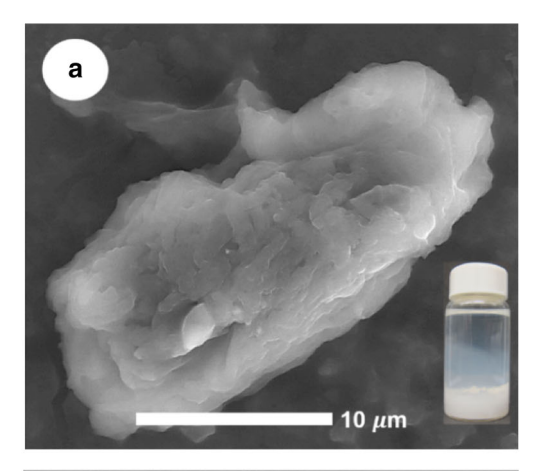
produced a smaller and narrower size distribution than the neutral condition (Fig. 4c). All in all, the dry ball milling pretreatment followed by the homogenization treatment failed to produce nanofibers.

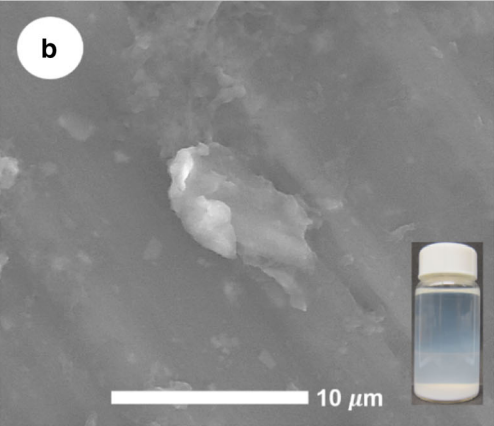
The wet milling followed by the high-pressure homogenization did produce ChNFs. Figure 5 displays the morphology and size distributions of the resulting ChNFs under the three conditions. The diameters (width) of the resulting ChNFs were analyzed by ImageJ software based on TEM images. Approximately one hundred nanofibers for each sample were measured, and the average diameters (width) and their size distributions are shown in Fig. 5b, d, and f. The length values of the resulting ChNFs were not obtained due to the difficulty in identifying both ends of the nanofibers on the TEM images. The wet milling and homogenization under the neutral condition produced the relatively coarse ChNFs with a diameter of around 19 nm and broad size distribution (Fig. 5a, b). The acidic homogenization produced the finer ChNFs with a diameter of around 16 nm and a relatively narrower size distribution (Fig. 5c, d). Further, both the acidic milling and acidic homogenization produced the finest ChNFs with a diameter of 11.9  $\pm$  6.3 nm and the narrowest size distribution (Fig. 5e, f). All resulting ChNFs formed stable suspensions beyond one-month storage (Fig. 5 insets). In general, the acidic condition helped surface cationization of chitin fibers resulting in the interfibrillar electrostatic repulsion force, which facilitated forming a much looser and opener fiber structure beneficial to the mechanical disintegration of chitin particles into ChNFs. Other researchers report the similar method to produce chitin- and chitosan nanofibers. For example, Liu et al. (2011, 2013a, b) has employed aqueous grinding pretreatment of chitin and chitosan using a conical grinder and then followed by high-pressure homogenization treatment to generate chitin and chitosan nanofibers, respectively. This wet grinding and mechanical disintegration of chitin in neutral medium generated relatively coarse networked chitin nanofibers with a diameter of about 50 nm. However, the influences of grinding and subsequent mechanical disintegration under acidic medium have











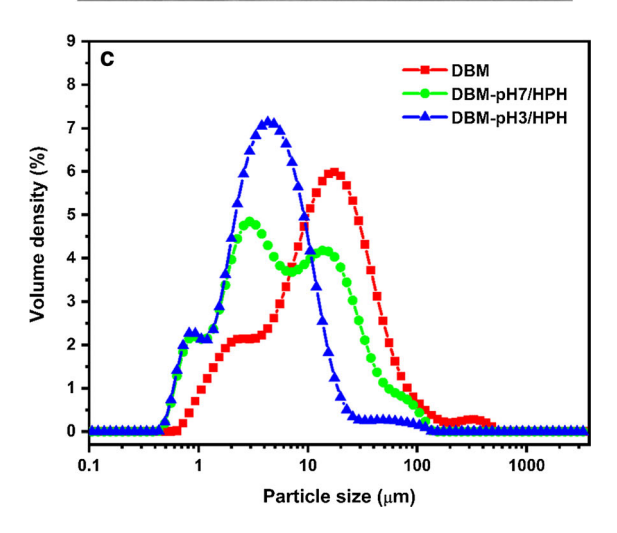
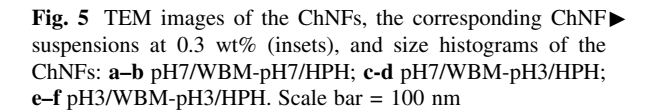


**Fig. 4** SEM images of the chitin products **a** DBM-pH7/HPH and **b** DBM-pH3/HPH (Inset: the corresponding chitin particle suspensions), and **c** particle size distribution

not been reported yet. This study demonstrated that wet ball mill grinding in acidic aqueous medium effectively pre-fibrillated chitin and produced finer



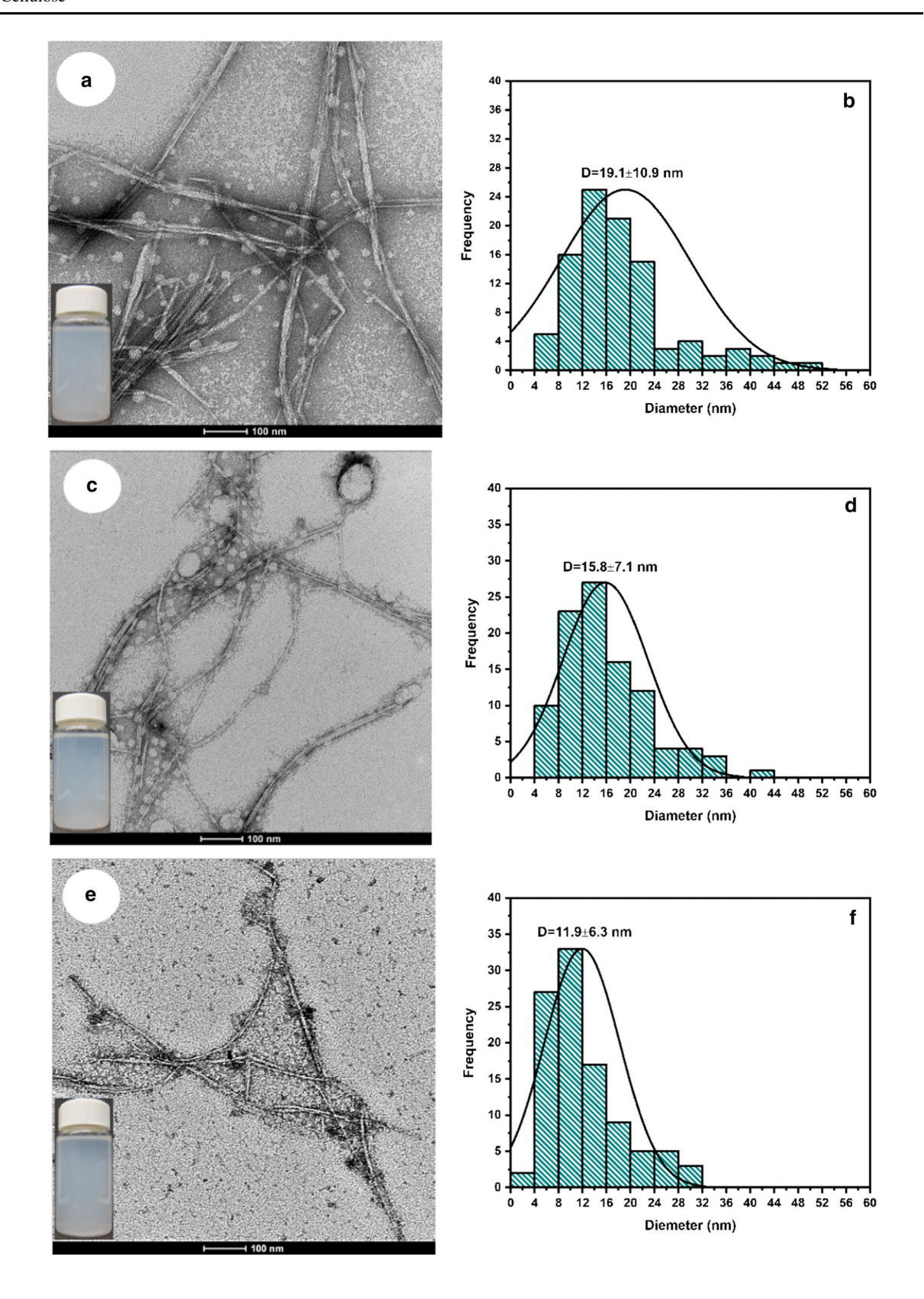
and smaller chitin nanofibers with a diameter of about 12 nm after high-pressure homogenization. It is believed that this effect was aided by the interfibrillar electrostatic repulsion forces that were induced by the protonation under acidic medium. It is interesting to note that a few spherical particles on the nanoscale observed on the TEM images might be some ball milling-induced broken but unfibrillated chitin. Some unknown white dots observed on the TEM images might be chitin nanoparticles, but most probably came from negative staining materials.

Effect of ball milling conditions on chemical structure and thermals stability

Figure 6 compares the FTIR spectra of the raw chitin and the resulting chitin microparticles and ChNFs. The band at 3447 cm<sup>-1</sup> was assigned to the intramolecular hydrogen bond O-H stretching, the bands at 3269 cm<sup>-1</sup> and 3104 cm<sup>-1</sup> to the asymmetric and symmetric stretching vibration of N-H, respectively, and the bands at 2933 cm<sup>-1</sup> and 2890 cm<sup>-1</sup> to the symmetric stretching vibration of -CH2 and asymmetric stretching vibration of - CH<sub>3</sub> in chitin molecule, respectively (Cárdenas et al. 2004). The two strong bands at 1662 cm<sup>-1</sup> and 1558 cm<sup>-1</sup> were assigned to the stretching of the C=O in the amide I and the overlapping of stretching of the C-N and the bending of the N-H in the amide II, respectively (Cárdenas et al. 2004; Rinaudo 2006). The shoulder at 1636 cm<sup>-1</sup> was a unique signature band for  $\alpha$ -chitin (Rinaudo 2006), which could not be found in  $\beta$ -chitin. The band at 1157 cm<sup>-1</sup> was attributed to the C-O-C glycosidic ether band arising from the polysaccharide components (Lu et al. 2015; Schwanninger et al. 2004). The band at 898 cm $^{-1}$  was ascribed to the  $\beta$ linkage in chitin (Cárdenas et al. 2004). The ball milling under either neutral or acidic conditions rendered similar characteristic bands discussed above to the raw chitin, indicating that the chemical structure was not altered under this treatment.

Figure 7 displays the typical TGA and DTG curves of the resulting chitin products obtained by the ball







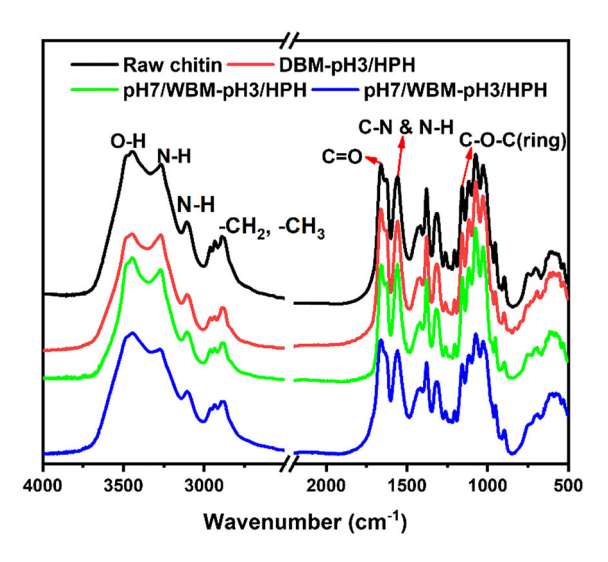
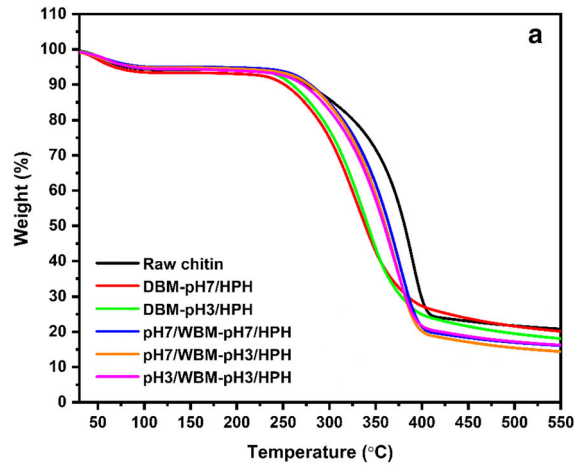


Fig. 6 FTIR spectra of raw chitin and the resulting chitin products

milling followed by the homogenization. The degradation temperature of 5% weight loss  $(T_{(5\%)})$  as a result of polymer degration after removing water loss, the onset degradation temperature (T<sub>(onset)</sub>) based on TGA curves, the degradation temperature of 50% weight loss ( $T_{(50\%)}$ ) and the peak temperature of DTG curves (T<sub>DTG peak</sub>) are summarized in Table S2. The original chitin exhibited the three main stages of weight loss (Fig. 7b). The first stage occurring between 50 and 110 °C was due to water evaporation; the second degradation took place at around 270 °C as a result of the decomposition of N-acetamido groups; the third degradation occurred at 390.6 °C, which was ascribed to the decomposition of the backbone of chitin (Kumar et al. 2013). The peak temperature at the DTG curve,  $T_{max}$ , is often regarded as an essential indicator of thermal stability corresponding to the maximum weight loss rate or the maximum decomposition rate (Liu et al. 2013a; Zhong et al. 2015). The particles obtained with the dry milling as a pretreatment had much lower  $T_{max}$  than that of the raw chitin, a reduction at around 55 °C, indicating a significant loss of thermal stability. However, there was around 20 °C reduction in  $T_{max}$  of the chitin nanofibers obtained using the wet ball milling as the pretreatment. Dry ball milling also resulted in much lower the T<sub>5%</sub> degradation temperature due to polymer (chitin) degradation and the onset thermal degradation temperature of the final products when compared to those obtained from wet ball milling pretreatment, as shown in Table S2. It



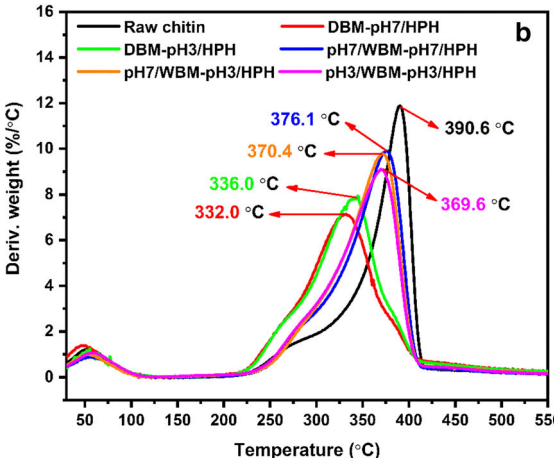
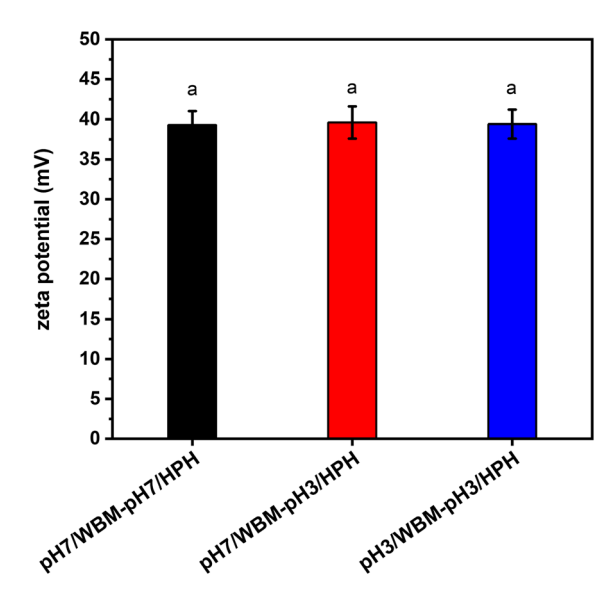


Fig. 7 TGA and DTG curves of raw chitin and the resulting chitin products

appears that the ball mill conditions, especially the dry or wet milling state, played a critical role in influencing the thermal stability of the final products. The effect of the wet ball milling pretreatment on the thermal stability was much less pronounced than that using the dry ball milling pretreatment. It may be ascribed mainly to the significant loss of the crystallinity under the dry milling. Low crystallinity may account for poor thermal stability of a product because less amount of energy is demanded to disrupt crystalline domains (Avolio et al. 2012; Pedersoli Júnior 2000).

Figure 8 shows the zeta potentials of all the three resulting ChNFs, there is no statistically significant difference among the different ChNFs. The zeta potentials for all the ChNFs were approximate 39 mV at the pH of 3, which might be mainly induced





**Fig. 8** The zeta potentials of the resulting ChNFs.The same lowercase letter indicates there is no statistically significant difference in zeta potentials between ChNF samples

by the protonation of the existing amino groups  $(-NH_2)$  in chitin molecules under the acidic condition into ammonium cations  $(-NH_3^+)$ . As discussed previously, chitin usually bears about 5-15% amino groups because of partial deacetylation often occurs during its extraction from shells under alkali conditions (Cárdenas et al. 2004; Pillai et al. 2009).

## Conclusion

This study demonstrated that wet ball milling could generate ChNF precursors with different degrees of pre-fibrillation, which were dependent on the pH (neutral or acidic) of the aqueous media. It was found that ball milling of chitin powder in a mildly acidic aqueous medium was the most effective in prefibrillating chitin to produce efficient ChNF precursors with the unchanged crystal structure and almost did not affect crystallinity. Individual chitin nanofibers, having an average diameter of around 12 nm, were successfully obtained by further mechanical disintegration of these ChNF precursors using high-pressure homogenization. Although ball milling under the dry state proved to be a powerful tool to reduce particle size, break down the crystalline structure, and decrease the crystallinity of chitin, however, no fibrous-morphology ChNFs were obtained in the subsequent mechanical disintegration step. The products obtained by wet ball milling pretreatment exhibited much higher thermal stability than those prepared with dry milling pretreatment. The results indicate that pre-fibrillation of chitin via ball milling in this study plays a crucial role in successful ChNF generation in a subsequent mechanical disintegration device; wet ball milling, especially under mildly acidic conditions, is a promising green approach to produce efficient precursors for ChNF production.

**Acknowledgments** This work was supported by the Center for Bioplastics and Biocomposites (CB<sup>2</sup>), a National Science Foundation Industry/University Cooperative Research Center (Awards IIP-1439732 & 1738669).

#### Compilance with ethical standards

**Conflict of interest** The authors declare that they have no conflict of interest.

#### References

Avolio R, Bonadies I, Capitani D et al (2012) A multitechnique approach to assess the effect of ball milling on cellulose. Carbohydr Polym 87:265–273. https://doi.org/10.1016/j.carbpol.2011.07.047

Butchosa N, Brown C, Larsson PT et al (2013) Nanocomposites of bacterial cellulose nanofibers and chitin nanocrystals: fabrication, characterization and bactericidal activity. Green Chem 15:3404–3413. https://doi.org/10.1039/c3gc41700j

Cárdenas G, Cabrera G, Taboada E, Miranda SP (2004) Chitin characterization by SEM, FTIR, XRD, and <sup>13</sup>C cross polarization/mass angle spinning NMR. J Appl Polym Sci 93:1876–1885. https://doi.org/10.1002/app.20647

Chauruka SR, Hassanpour A, Brydson R et al (2015) Effect of mill type on the size reduction and phase transformation of gamma alumina. Chem Eng Sci 134:774–783. https://doi.org/10.1016/j.ces.2015.06.004

Fan Y, Saito T, Isogai A (2008) Chitin nanocrystals prepared by TEMPO-mediated oxidation of α-chitin. Biomacromolecules 9:192–198

Goodrich JD, Winter WT (2007) α-chitin nanocrystals prepared from shrimp shells and their specific surface area measurement. Biomacromolecules 8:252–257. https://doi.org/10.1021/bm0603589

Ifuku S, Nogi M, Yoshioka M et al (2010) Fibrillation of dried chitin into 10–20 nm nanofibers by a simple grinding method under acidic conditions. Carbohydr Polym 81:134–139. https://doi.org/10.1016/j.carbpol.2010.02. 006

Ifuku S, Morooka S, Nakagaito AN et al (2011) Preparation and characterization of optically transparent chitin nanofiber/



- (meth) acrylic resin composites. Green Chem 13:1708–1711. https://doi.org/10.1039/c1gc15321h
- Kumar MNVR (2000) A review of chitin and chitosan applications. React Funct Polym 46:1–27. https://doi.org/10.1016/S1381-5148(00)00038-9
- Kumar NA, Rejinold NS, Anjali P et al (2013) Preparation of chitin nanogels containing nickel nanoparticles. Carbohydr Polym 97:469–474. https://doi.org/10.1016/j.carbpol. 2013.05.009
- Lee H, Mani S (2017) Mechanical pretreatment of cellulose pulp to produce cellulose nanofibrils using a dry grinding method. Ind Crop Prod 104:179–187. https://doi.org/10. 1016/j.indcrop.2017.04.044
- Li M-C, Wu Q, Song K et al (2015) Cellulose nanoparticles: structure—morphology—rheology relationships. ACS Sustain Chem Eng 3:821–832. https://doi.org/10.1021/acssuschemeng.5b00144
- Liu D, Chang PR, Chen M et al (2011) Chitosan colloidal suspension composed of mechanically disassembled nanofibers. J Colloid Interface Sci 354:637–643. https://doi.org/ 10.1016/j.jcis.2010.11.041
- Liu D, Sun X, Tian H et al (2013a) Effects of cellulose nanofibrils on the structure and properties on PVA nanocomposites. Cellulose 20:2981–2989. https://doi.org/ 10.1007/s10570-013-0073-6
- Liu D, Zhu Y, Li Z, Tian D et al (2013b) Chitin nanofibrils for rapid and efficient removal of metal ions from water system. Carbohydr Polym 98:483–489. https://doi.org/10. 1016/j.carbpol.2013.06.015
- Lu Q, Lin W, Tang L et al (2015) A mechanochemical approach to manufacturing bamboo cellulose nanocrystals. J Mater Sci 50:611–619. https://doi.org/10.1007/s10853-014-8620-6
- Minke R, Blackwell J (1978) The structure of α-chitin. J Mol Biol 120:167–181. https://doi.org/10.1016/0022-2836(78)90063-3
- Missoum K, Belgacem MN, Bras J (2013) Nanofibrillated cellulose surface modification: a review. Materials (Basel) 6:1745–1766. https://doi.org/10.3390/ma6051745
- Nair GK, Dufresne A (2003) Crab shell chitin whisker reinforced natural rubber nanocomposites. 1. processing and swelling behavior. Biomacromol 4:657–665. https://doi.org/10.1021/bm020127b
- Nakagawa YS, Oyama Y, Kon N et al (2011) Development of innovative technologies to decrease the environmental burdens associated with using chitin as a biomass resource: mechanochemical grinding and enzymatic degradation. Carbohydr Polym 83:1843–1849. https://doi.org/10.1016/ j.carbpol.2010.10.050
- Nemoto S, Ueno T, Watthanaphanit A et al (2017) Crystallinity and surface state of cellulose in wet ball-milling process. J Appl Polym Sci 44903:1–7. https://doi.org/10.1002/app. 44903
- Pedersoli Júnior JL (2000) Effect of cellulose crystallinity on the progress of thermal oxidative degradation of paper. J Appl Polym Sci 78:61–66

- Pillai CKS, Paul W, Sharma CP (2009) Chitin and chitosan polymers: chemistry, solubility and fiber formation. Prog Polym Sci 34:641–678. https://doi.org/10.1016/j. progpolymsci.2009.04.001
- Qing Y, Sabo R, Zhu JY et al (2013) A comparative study of cellulose nanofibrils disintegrated via multiple processing approaches. Carbohydr Polym 97:226–234. https://doi.org/10.1016/j.carbpol.2013.04.086
- Rinaudo M (2006) Chitin and chitosan: properties and applications. Prog Polym Sci 31:603–632. https://doi.org/10.1016/j.progpolymsci.2006.06.001
- Salaberria AM, Fernandes SCM, Diaz RH, Labidi J (2015) Processing of α-chitin nanofibers by dynamic high pressure homogenization: characterization and antifungal activity against *A. niger*. Carbohydr Polym 116:286–291. https://doi.org/10.1016/j.carbpol.2014.04.047
- Schwanninger M, Rodrigues JC, Pereira H, Hinterstoisser B (2004) Effects of short-time vibratory ball milling on the shape of FT-IR spectra of wood and cellulose. Vib Spectrosc 36:23–40. https://doi.org/10.1016/j.vibspec.2004.02.003
- Shams MI, Ifuku S, Nogi M et al (2011) Fabrication of optically transparent chitin nanocomposites. Appl Phys A Mater Sci Process 102:325–331. https://doi.org/10.1007/s00339-010-5969-5
- Suenaga S, Totani K, Nomura Y et al (2017) Effect of acidity on the physicochemical properties of α- and β-chitin nanofibers. Int J Biol Macromol 102:358–366. https://doi.org/10.1016/j.ijbiomac.2017.04.011
- Venkataraman KS, Narayanan KS (1998) Energetics of collision between grinding media in ball mills and mechanochemical effects. Powder Technol 96:190–201
- Willart JF, Descamps M (2008) Solid state amorphization of pharmaceuticals. Mol Pharm 5:905–920
- Yan N, Chen X (2015) Don't waste seafood waste: Turning castoff shells into nitrogen-rich chemicals would benefit economies and the environment. Nature 524:155–157
- Zhang L, Tsuzuki T, Wang X (2015) Preparation of cellulose nanofiber from softwood pulp by ball milling. Cellulose 22:1729–1741. https://doi.org/10.1007/s10570-015-0582-6
- Zhong T, Oporto GS, Jaczynski J, Jiang C (2015) Nanofibrillated cellulose and copper nanoparticles embedded in polyvinyl alcohol films for antimicrobial applications. Biomed Res Int 2015:1–8
- Zhong T, Wolcott MP, Liu H, Wang J (2019) Developing chitin nanocrystals for flexible packaging coatings. Carbohydr Polym 226:115276. https://doi.org/10.1016/j.carbpol. 2019.115276
- **Publisher's Note** Springer Nature remains neutral with regard to jurisdictional claims in published maps and institutional affiliations.

